


## RESEARCH ARTICLE

# Microstates in complex and dynamical environments: Unraveling situational awareness in critical helicopter landing maneuvers

Camila S. Deolindo<sup>1</sup> | Mauricio W. Ribeiro<sup>1</sup> | Maria A. A. de Aratanha<sup>1</sup> |  
 José R. S. Scarpari<sup>2,3</sup> | Carlos H. Q. Forster<sup>2</sup> | Roberto G. A. da Silva<sup>2</sup> |  
 Birajara S. Machado<sup>1</sup> | Edson Amaro Junior<sup>1,4</sup> | Thomas König<sup>5</sup> | Elisa H. Kozasa<sup>1</sup> 

<sup>1</sup>Hospital Israelita Albert Einstein, São Paulo, Brazil

<sup>2</sup>Instituto Tecnológico de Aeronáutica, São José dos Campos, Brazil

<sup>3</sup>Instituto de Pesquisas e Ensaio em Voos (IPEV), São José dos Campos, Brazil

<sup>4</sup>Hospital das Clínicas, University of São Paulo Medical School, São Paulo, Brazil

<sup>5</sup>University Hospital of Psychiatry, Bern, Switzerland

## Correspondence

Elisa H. Kozasa, Hospital Israelita Albert Einstein, São Paulo, Brazil.  
 Email: ehkozasa@gmail.com

## Funding information

Conselho Nacional de Desenvolvimento Científico e Tecnológico (CNPq); Coordenação de Aperfeiçoamento de Pessoal de Nível Superior (CAPES); Instituto de Pesquisas e Ensaio em Voo (IPEV); Instituto Israelita de Ensino e Pesquisa Albert Einstein (IIEPAE); PRONUIEMP

## Abstract

Understanding decision-making in complex and dynamic environments is relevant for designing strategies targeting safety improvements and error rate reductions. However, studies evaluating brain dynamics in realistic situations are scarce in the literature. Given the evidence that specific microstates may be associated with perception and attention, in this work we explored for the first time the application of the microstate model in an ecological, dynamic and complex scenario. More specifically, we evaluated elite helicopter pilots during engine-failure missions in the vicinity of the so called “dead man’s curve,” which establishes the operational limits for a safe landing after the execution of a recovery maneuver (autorotation). Pilots from the Brazilian Air Force flew a AS-350 helicopter in a certified aerodrome and physiological sensor data were synchronized with the aircraft’s flight test instrumentation. We assessed these neural correlates during maneuver execution, by comparing their modulations and source reconstructed activity with baseline epochs before and after flights. We show that the topographies of our microstate templates with 4, 5, and 6 classes resemble the literature, and that a distinct modulation characterizes decision-making intervals. Moreover, the source reconstruction result points to a differential activity in the medial prefrontal cortex, which is associated to emotional regulation circuits in the brain. Our results suggest that microstates are promising neural correlates to evaluate realistic situations, even in a challenging and intrinsically noisy environment. Furthermore, it strengthens their usage and expands their application for studying cognition under more realistic conditions.

## KEYWORDS

aircraft, awareness, brain mapping, electroencephalography, empirical research, task performance and analysis

This is an open access article under the terms of the Creative Commons Attribution-NonCommercial-NoDerivs License, which permits use and distribution in any medium, provided the original work is properly cited, the use is non-commercial and no modifications or adaptations are made.

© 2021 The Authors. *Human Brain Mapping* published by Wiley Periodicals LLC.

## 1 | INTRODUCTION

Failures, accidents or incidents involving complex systems are not solely linked to equipment malfunction, but also to human (mis) behavior or judgmental errors. The increase in equipment complexity generally requires more training, precision, or even the coordination of multiple individuals. Therefore, during product development and interface design, one must account for the operator's cognitive and psychomotor abilities in an effort to reduce error rates. In this context, Situational Awareness (SA) consolidated as a major research field within Human Factors, and explores the pivotal role of the operator in the overall system performance (Endsley, 2000). According to Endsley (1995), the concept of SA is more than "merely looking at various pieces of information," since it also encompasses the cognitive processes that attribute meaning to temporal and spatial cues, and their usage to extrapolate to future scenarios. Thus, SA combines pattern recognition, analysis, narrative composition and metacognitive processes at different times; and concerns how the individual attributes meaning to the environment (Endsley, 2000). Several approaches have already been proposed to quantify the SA of the operator (Charles & Nixon, 2019; Endsley & Garland, 2000), but, so far, little is known about the cognitive processes and the robustness of their potential neural correlates outside of controlled environments.

Endsley (2000) differentiates the cognitive process used to obtain SA, that is, the active process of acquiring information (Situation Assessment), from the resulting state per se, and a promising field is to explore whether these processes are also distinct or how they integrate from a physiological point of view. Thus, microstates are interesting neural correlates to characterize SA in critical situations, due to evidence that attentional and perceptual networks neural correlates may be distinguishable from one another (Bréchet et al., 2019; Seitzman et al., 2017), which would enable the assessment of the dynamics of these network during decision-making processes.

Under this construct, the electroencephalogram (EEG) is represented as a series of stable and recurring topographic patterns over time, which result from the synchronized activity of spatially distributed electrical sources (Khanna, Pascual-Leone, Michel, & Farzan, 2015). These periods of stability or microstates are interpreted as corresponding to different functional states of the brain and its fundamental blocks of information processing (Lehmann, Ozaki, & Pal, 1987). Thus, according to this model, microstates are electrophysiological correlates of the coordinated activity of different neuronal assemblies, such that changes in topographies are representative of the overall modifications in neuronal activity coordination over time (Michel & Koenig, 2018). Hence, it is possible to study the interaction of the individual with the environment, by assessing its internal states on a millisecond scale (Koenig et al., 2002).

A myriad of evidences reinforce that microstates are emergent properties of the EEG signal. The recurring topographies display characteristic patterns, already reported in several studies in the literature (Michel & Koenig, 2018). These patterns are recovered not only on healthy individuals but also on diverse groups of patients (Rieger, Hernandez, Baenninger, & Koenig, 2016), and they are preserved

through aging, with modifications in dynamic parameters that are compatible with the different development stages of an individual over time (Koenig et al., 2002). Furthermore, the dynamic modulation of microstates is related to behavior and perception (Britz, Díaz Hernández, Ro, & Michel, 2014; Britz & Michel, 2011; Müller et al., 2005; Pedroni et al., 2017), may be affected in some diseases (da Cruz et al., 2020; Dierks et al., 1997; Khanna et al., 2015; Rieger et al., 2016; Strik et al., 1997), by the use of specific medications (Khanna et al., 2015; Kinoshita et al., 1995) and in altered states of consciousness (Bréchet, Brunet, Perogamvros, Tononi, & Michel, 2020; Katayama et al., 2007; Khanna et al., 2015).

Previous attempts to assign a functional meaning to microstate classes have established associations with Resting State Networks (RSN). The hypothesis is that RSN dynamics is, in fact, much faster than what is inferred from functional magnetic resonance imaging (fMRI) studies and that the microstates would be their electrophysiological signature (Britz, Van De Ville, & Michel, 2010; Michel & Koenig, 2018; Van De Ville, Britz, & Michel, 2010). Despite the body of evidence suggesting a close relationship between microstates and specific cognitive functions (Michel & Koenig, 2018), only recently the dynamic modulations during cognitive tasks, the possible influence of mental contents (Bréchet et al., 2019; Milz et al., 2016; Pedroni et al., 2017; Seitzman et al., 2017) and individual expertise (Panda et al., 2016) have been explored.

In this work, we explore for the first time the application of the microstate model in an ecological, dynamic and complex scenario to access neurophysiology and cognition, that is, we investigate if these neural correlates are recovered in a naturalistic and unconstrained environment and whether their modulations provide further insights about the task. More specifically, we evaluated high performance helicopter pilots during engine failure missions, performing the Autorotation (AR) maneuver. The AR is defined as a flight state in which the helicopter rotor no longer moves due to the engine, but due to the action of air rising towards it. At this point, the pilot must lower the collective, an action which decouples the engine shaft from the rotor shaft, and guide the aircraft through a safe landing. The AR maneuver is part of standard piloting training, since it is an emergency landing procedure in the event of engine or tail rotor failures (Federal Aviation Administration, 2016; Jingze, 2011; Johnson, 2012). However, there is a set of flight conditions in which the execution of the AR maneuver and landing becomes exceedingly difficult or hazardous, and, therefore, the operation of the aircraft is restricted to avoid them. These conditions are mapped using a height versus speed diagram, and the curve that limits the operating regions is known as the "dead man's curve," height-speed curve or height-speed envelope (Federal Aviation Administration, 2016; Jingze, 2011; Johnson, 2012). Currently, the curve is theoretically computed as a function of energy dissipation (potential and kinetic) into the rotor rotation, but in practical terms, these limits are assessed on several flight tests, and they can be largely influenced by subjective criteria. However, the large number of accidents due to improper maneuver execution motivate the exploration of objective and physiological-based methods to help the establishment of safety parameters: According to reports of the The United

States Joint Helicopter Safety Analysis Team (2011, 2014a, 2014b), ARs during practice and emergency were the second top causes of accidents in the years of 2000, 2001 and 2006 (31.7%) and from 2009 to 2011 (32.8%), accounting for a statistically significant proportion of fatal accidents.

Therefore, the primary goal of this work was to assess the feasibility of the microstate model in a challenging scenario, and to contrast the degree of similarity to those of experiments performed under controlled circumstances. More specifically, our secondary goal was to explore the microstate modulations during AR maneuvers performed in the vicinity of the dead man's curve. Our hypothesis was that the parameters of Microstate D (duration, occurrence and coverage), associated with the attention and cognitive control networks, would be higher during the maneuver performance as opposed to the rest condition.

## 2 | METHODS

### 2.1 | Ethics

This work was approved by the ethics committee of the Hospital Israelita Albert Einstein (CAAE 72744717.7.0000.0071). All volunteers agreed to participate and signed an informed consent form. We emphasize that, although this project involves risks for the participants, they would already perform this set of maneuvers as part of a special mission within the scope of their professional activities and our project involved only the additional sensing and monitoring of their physiological responses.

### 2.2 | Experimental description

The flight campaign was performed in São José dos Campos, Brazil, in a certified aerodrome. The AS-350 helicopter is owned by the Brazilian Air Force and has capacity for six (6) occupants. The aircraft was equipped with a flight test instrumentation (FTI), to capture flight parameters such as altitude, angular speeds and

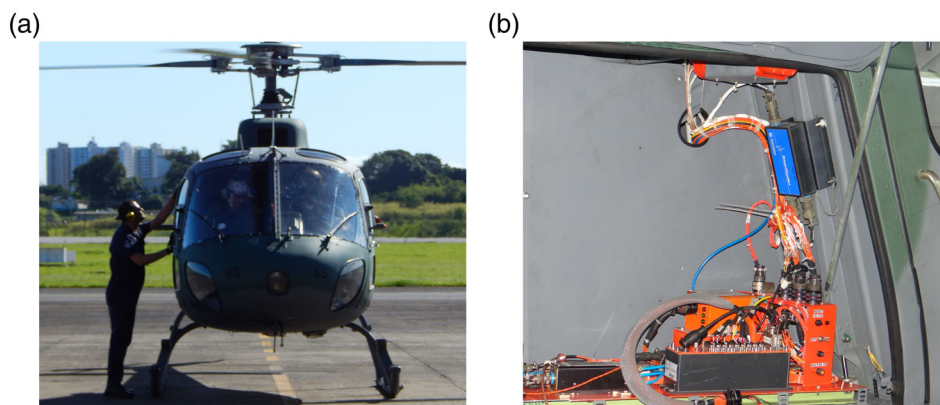
acceleration. It also encompassed sensing in several systems and instruments, such as flight controls and the rotor-fuselage proximity. All information was synchronized and sampled at 64 Hz (Figure 1).

We collected data from eleven (11) pilots from the Brazilian Air Force and Army, all males and very experienced in piloting but with different expertise in AR, as shown in Table 1. Our sample was composed of seven (7) test pilots and four (4) helicopter instructors. All pilots undergo annual check-ups and were considered healthy at the time of the study.

The crew encompassed a test pilot that was in command of the aircraft, a flight instructor in supervision, and a flight test engineer in flight coordination. Furthermore, a flight safety specialist supervised the campaign planning, an instrumentation specialist managed the aircraft systems and a specialized maintenance team was on duty. The maneuver points were pre-selected in order to scan the vicinity of the dead man's curve, as shown in Figure 2. Since the campaign was based on simulated engine failures, the engine was not completely off but had its power reduced until the aircraft lost lift. Maneuver abortion was always available. The engine-failure simulations were always performed on safe altitudes and, at the end, the engine was rekindled in flight. Pilot fatigue patterns were constantly assessed. As part of the operational routine, the crew met before each flight to review the mission planning (*briefing*), and at the end (*debriefing*), to review the execution.

Regarding the physiology, we collected signals from EEG, heart-beat, breathing, electrodermal activity and from the left triceps (EMG), given that the left arm is employed to control the aircraft collective. All sensors were sampled at 500 Hz (Brain Products, Gilching DE). The physiological signal acquisition was synchronized by a push button trigger, pressed by the flight engineer immediately before each maneuver. In addition, the pilot's eye movement was recorded by an Eye tracker system (Tobii) and his facial expression was recorded with high resolution cameras. In this work, we analyze only the EEG data.

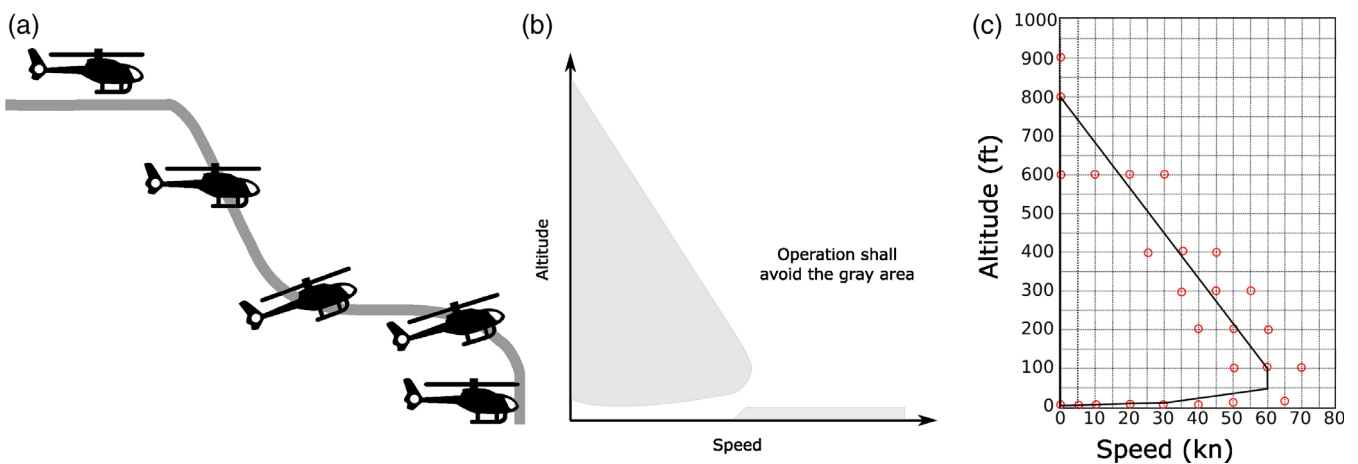
The EEG was acquired with the Brain Products LiveAmp 32 active channel setup, because the amplifier is portable, has integrated accelerometers and is already designed for experiments subject to movement. The impedance was kept below 25 k $\Omega$  and the electrodes were positioned following the 10/20 standard.



**FIGURE 1** Pictures of the aircraft and of the flight test instrumentation. (a) Aircraft AS-350; (b) part of the data acquisition system in the right luggage compartment

**TABLE 1** Description of the sample: Age and expertise of each pilot

ID	Age	Total flight hours			Instructor AS-350	Test pilot
		Total	Helicopter	AS-350		
Sub 01	41	4,006:05	2,660:40	1,441:00	Yes	Yes
Sub 02	37	2,592:25	2,337:20	1,740:55	Yes	Yes
Sub 03	37	3,308:40	1,411:25	178:35	No	Yes
Sub 04	38	1,746:45	1,588:30	133:20	No	Yes
Sub 05	46	3,500:10	1,988:30	1,479:15	Yes	Yes
Sub 06	48	3,730:10	2,580:30	1,725:10	Yes	Yes
Sub 07	37	1,755:45	1,755:45	1,430:00	No	Yes
Sub 08	37	2,242:40	1,037:10	234:20	No	No
Sub 09	35	1,384:00	1,219:20	722:55	No	No
Sub 10	41	2,750:35	2,155:00	1,120:50	No	No
Sub 11	42	3,650:05	2,350:40	1,130:00	No	No

**FIGURE 2** Schematic representation of the AR maneuver (a) and the Dead Man's Curve (b). Diagram (b) shows combinations of height and speed where the operation shall be avoided. In (c), we display the selected maneuver test points used in this campaign, spanning the vicinity of the flight envelope. Source: Adapted from Federal Aviation Administration (2016). For a video of a maneuver execution, the reader is referred to the Supplementary Material

We assembled a temporary acquisition lab in a quiet room, annex to the aircraft hangar. The walking distance from the room to the landed helicopter was on the order of 5 min. There we collected baseline data from the participants immediately before and after each flight. In both cases, the participants were instructed to remain with eyes open for a minute while gazing at a cross projected on a screen in front of them, relaxing and trying not to move.

The physiological data acquisition started a few moments before takeoff and was only resumed after landing. Only segments around the AR maneuvers were analyzed. These epochs were centered at time points defined by the combination of the manual flight trigger with additional data from the FTI system: we selected the first instant after the trigger that indicated an engine power below 65%. We requested the pilots to avoid talking during the time windows around the maneuvers, to reduce EEG contamination.

We recall that there were different test points around the dead man's curve (Figure 2c), which relate to distinct difficulty

levels. Furthermore, additional test points, premeditated by the crew, were also introduced without previous awareness of the pilot. However, in the context of electrophysiology studies, there were few trial repetitions for each test point, and a low number of participants. Thus, in order to increase the final statistical power, the differences between test points were disregarded on the analyses.

## 2.3 | EEG preprocessing

For each maneuver execution, we segmented the EEG data in a 1-min window around the engine failure. Next, the data for ARs and baselines were pre-processed in BrainVision Analyzer version 2.1.0.137. Initially, we performed a semi-automatic inspection of the data, to exclude discontinuous sections due to movement artifacts from the volunteer or the wiring.

After that, all data sets (around the maneuver or during rest) were filtered with a Butterworth bandpass filter (0.5–50 Hz), with no phase lags and with a notch filter at 60 Hz (both of fourth order). Then, we performed a semi-automatic Independent Component Analysis (ICA). This method is traditionally used for ocular and muscular artifact extraction; however, it also efficiently characterized additional noise signatures during the flight. In order to reduce the amount of discarded components and, consequently, to avoid an excessive data dimensionality reduction, we further restricted the data epochs. Thus, the microstate analysis focused on the interval of  $-2$  to  $3$  s around the engine failure, since this is the decision-making time-window. Therefore, although the ICA was computed in 60 s segments, only the components characterizing noise within  $-2$  to  $3$  s were disregarded. Finally, the channels were referenced with respect to their average value. The pre-processing strategy was depicted in Figure 3.

## 2.4 | Microstate analysis

In this work, we performed microstate analysis using the plugin implemented by Thomas König, version 1.2, available at <http://www.thomaskoenig.ch>, combined with the EEGLAB toolbox version 14.1.2 (Delorme & Makeig, 2004).

In this framework, characteristic microstate topographies are initially computed at the level of an individual dataset, corresponding to centroids of a modified *K-means* classifier. This classifier is largely employed in the literature (Michel & Koenig, 2018). However, clustering algorithms such as the *K-means* have unstable results when fed with a small amount of data to discriminate patterns. Thus, in order to increase the power of the classifier, we concatenated all maneuver segments from each specific participant, even if they have been acquired in distinct flights. The same consideration was applied to

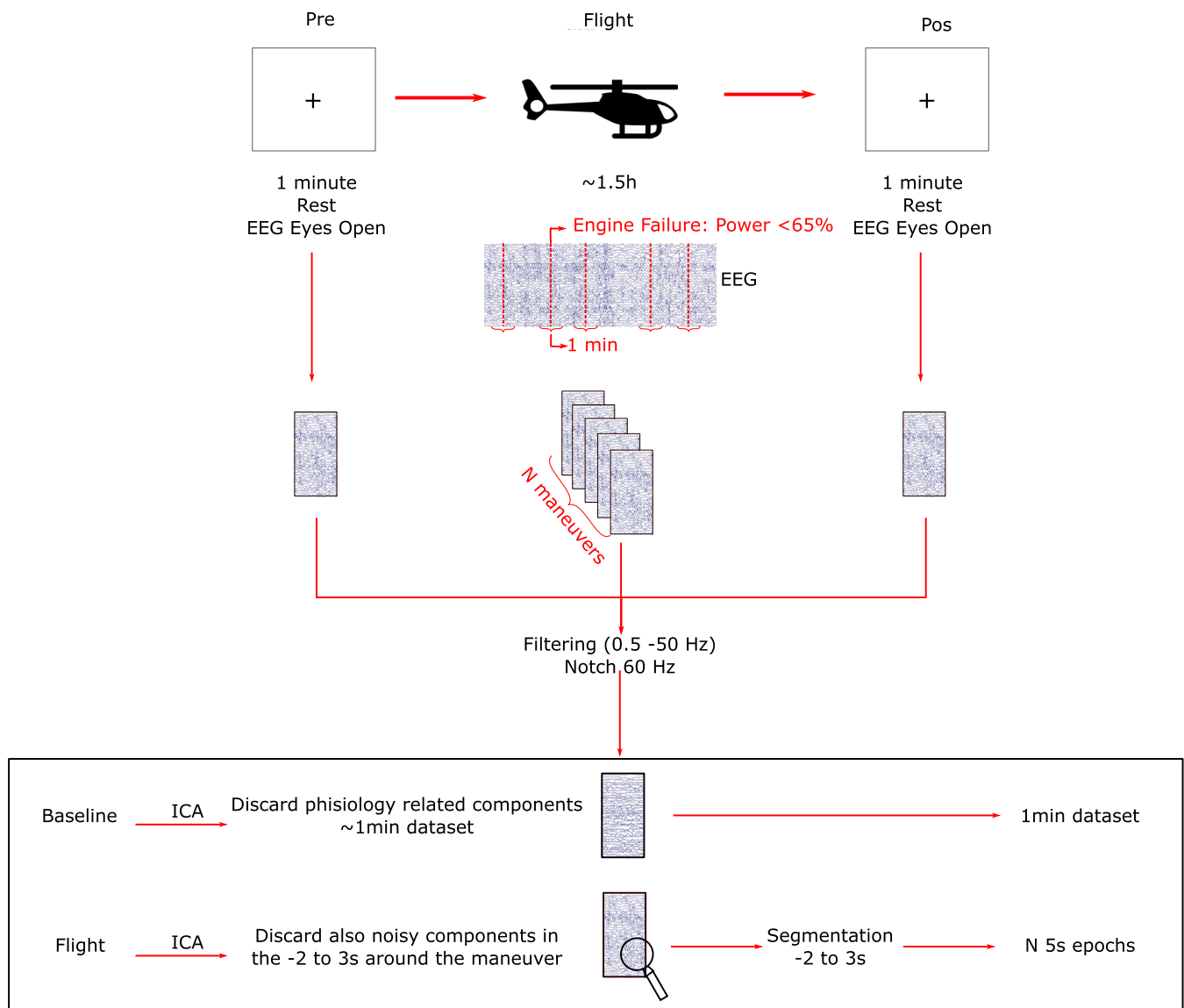


**FIGURE 3** EEG preprocessing schematics: While the baseline data was used to its full extent, the flight data was pruned around the engine failure, in order to restrict the artifact influences

resting data. Thus, characteristic templates on the subject level were computed based on three concatenated datasets: two related to resting data before and after flights and one representative of all AR maneuvers performed by the individual over the entire flight campaign.

These concatenated data result in a total of  $M$  microstate templates for each individual. However, their sequence in each individual and their correspondence is, at first, random. Therefore, the next step is to create a mean template, also with  $M$  maps, but at the group level. Here they are reordered such as to maximize the common variance between participants (Koenig et al., 1999). In this way, we calculated three sets of mean templates, with  $M$  maps, corresponding to the experimental conditions of interest: Rest before (RSpre) and after the flight (RSpos) and during the execution of the maneuvers (Flight).

After that, the reordering step was repeated, such as to compute second level templates out of these three conditions, generating a “Grand Mean” template, also with  $M$  topographies. Once again, they were randomly sorted and, to facilitate comparisons with the literature, they were reordered based on the normative reference of Koenig et al. (2002), computed out of data from 496 individuals, between 6 and 80 years old. The final step was to estimate the microstates' dynamic parameters. However, this is largely dependent on the referential template used for backfitting. The toolbox enables several template possibilities, ranging from the ones at the individual level, that is, computed exclusively from the participant data; at group level, considering all participants; and using a normative reference. We opted to consider the “Grand Mean,” the average template computed out of the data ensemble of our participants in all experimental conditions (RSpre, Flight, RSpos). The dynamic parameters were computed with 4, 5, and 6 classes of microstates, as they present interesting results in comparison with the literature.

In addition to the dynamic parameters of the microstates (duration, occurrence and coverage), the toolbox also computes the transition ratio between different classes. However, since the most frequent microstates have more transitions, these ratios are skewed measures, dependent upon the total number of occurrences of each class. Thus, in the toolbox, the output is corrected to consider the expected value for the transitions corrected by the occurrences.

Finally, the optimal number of microstate classes was computed using the predictive residual variance as defined by Pascual-Marqui, Michel, and Lehmann (1995), through the implementation of Poulsen, Pedroni, Langer, and Hansen (2018).

### 2.4.1 | Microstates: Statistics

In this experiment, our data had a hierarchical structure, that is, the repeated measures were always nested for the participants. Thus, for the statistical analysis, we employed a linear mixed effect model to account for both fixed and random effects, as described below, using the notation of Wilkinson and Rogers (1973), where  $MSparam$  corresponds to the value of the microstate parameter,  $Condition$  is

associated with the three analyzed moments (RSpre, Flight or RSpos) and  $Subject$  is the weight associated with the participants.

$$MSparam \sim 1 + Condition + (1|Subject) \quad (1)$$

The analysis was performed using the Statistics and Machine Learning toolbox from Matlab®. The model's parameters estimative employed the maximum restricted likelihood (REML), in order to avoid variance biases in the model. The residuals' normality hypothesis was assessed through a quantile–quantile graph and through the Shapiro–Wilk test. When the distribution violated normality, we inserted a logarithm operator in the dependent variable  $MSparam$ , in Equation (1).

## 2.5 | Source reconstruction analysis

The standard Low Resolution Brain Electromagnetic Tomography (sLORETA) algorithm was adopted for source reconstruction analysis, using the Key-LORETA software, version 20190617 and available at <http://www.uzh.ch/keyinst/loreta.htm>. This implementation uses the MNI152 template for head modeling (Mazziotta et al., 2001) and restricts its brain volume to gray matter regions, as advocated by the Tailarach probabilistic atlas (Lancaster et al., 2000). The volume is further divided into 6,239 voxels of 5 mm<sup>3</sup>. The source reconstruction algorithm was fed with the cluster maps of each subject referring to the three moments of interest (rest before and after the flight and during the maneuver—RSpre, Flight and RSpos). The sLORETA was applied to the first main component of the EEG momentary topographies, corresponding to the Global Field Power (GFP) peaks of each participant. The total power of the data was then subject-wise normalized, through one of the normalization options available at the software.

Our goal was to highlight areas with greater activity in flight in comparison to the baseline. Therefore, we computed a paired  $t$  test, contrasting the result of the maneuver (Flight) with baseline before flight (RSpre) for each class of microstates and used the contrast between the two resting conditions (RSpos – RSpre) as a control. For controlling false positives, we employed the Statistical non-Parametric Mapping feature (Nichols & Holmes, 2002).

## 3 | RESULTS

### 3.1 | Feasibility: Artifacts

The main objective of this study was to ensure the EEG feasibility during the adverse circumstances of helicopter piloting on AR: in addition to more prominent artifacts (e.g., sweat and movement), we also had to deal with the presence of harmonics corresponding to the aircraft's structural vibration modes and engine-related noise.

A large portion of these artifacts could be attenuated by simply transforming the EEG reference to the mean of all channels, given that several spurious sources affected the entire head homogeneously.

This is exemplified in Figure 4a, through the spectral data of one participant at flight and at rest. Moreover, the ICA targeting a window of interest, around the engine failure, was an attempt to compromise between preserving a data segment large enough to characterize the cognitive decision-making process, but to avoid discarding a very large amount of Independent Components (ICs), which could impair the resulting signal quality. This approach efficiently characterized artifacts, as exemplified in Figure 4b,c. This strategy allowed approximately 95% of the recorded maneuvers (219/232) to proceed to the later stages of analysis, albeit with reduced dimensionality (in the worst case it decreased from 32 to 23—Table S1). The main cause of maneuver data exclusions (13/232) were motion artifacts that could not be filtered. In addition, other important factors that reduced the amount of maneuvers were failures in the physiological setup (1 flight), and aircraft issues that required a premature interruption of the flight

plan or impaired the initial project schedule, such as structural damage and fire on the battery.

A final piece of evidence that highlights the success of the artifact removal strategy emerges from the results of the microstate analysis itself. It is possible to verify that the computed microstate templates are congruent with the literature, even when we change the number of classes, as evidenced below.

### 3.2 | Microstate analysis

After preprocessing, we followed the microstate analysis pipeline, computing microstate templates corresponding to each of the three experimental conditions—resting state prior to (RSpre) and after the flight (RSpos), during the AR maneuver (Flight)—in addition to the

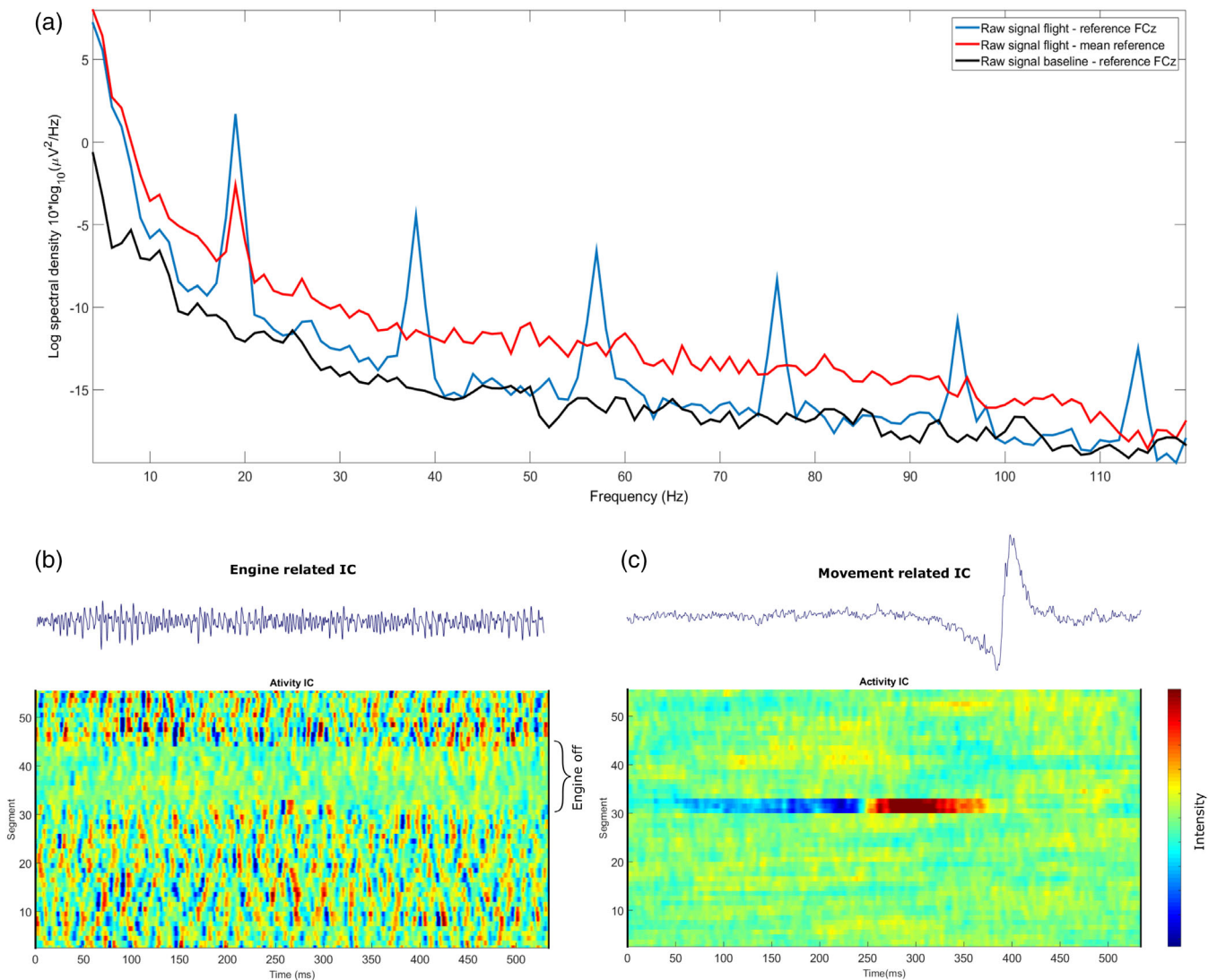
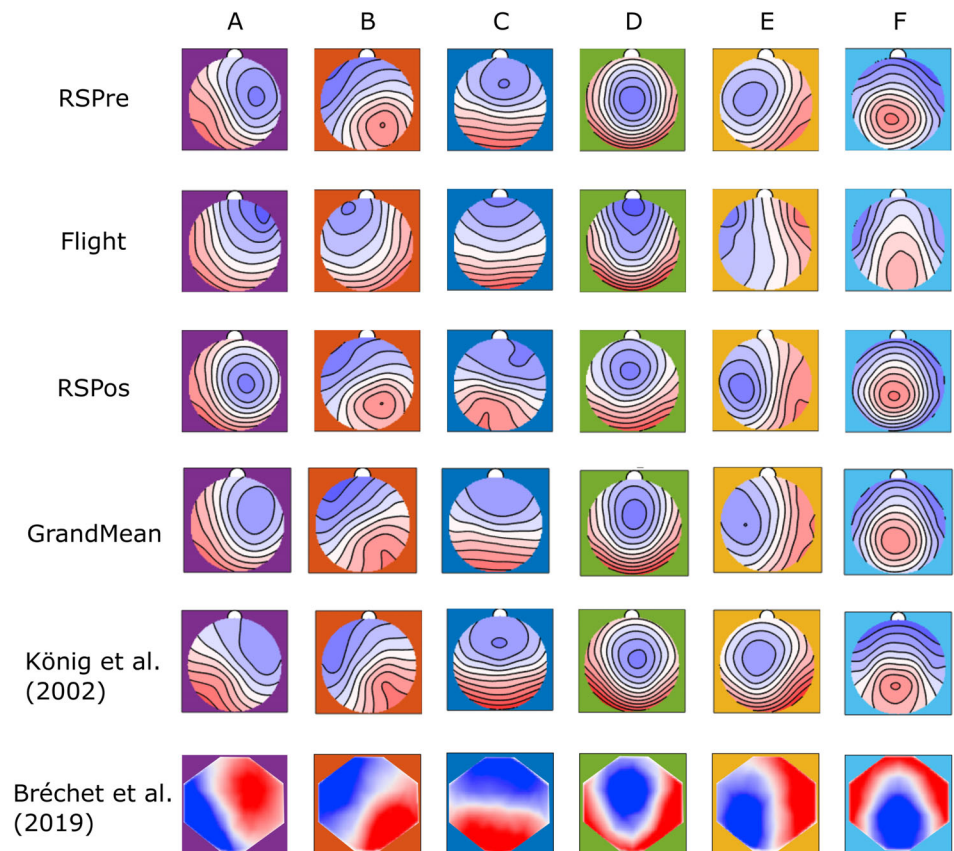


**FIGURE 4** EEG and artifacts: (a) Change of reference reduces the aircraft's structural vibration modes in the spectrum, as displayed by raw signal in the Cz electrode before and at flight. Some illustrative artifacts characterized by ICA are displayed in (b) and (c). We selected 1-min characteristic segments of the corresponding IC activity. The data was segmented to facilitate visualization. The engine failure occurs around segment 30. (b) Displays a component associated with the engine, whose activity assumes periodic patterns, that ceases when the engine is off. (c) Illustrates a component associated with the participant movement, characterized by a short-duration peak

**FIGURE 5** Mean microstate templates considering a total of six (6) classes during the three conditions (baseline before flight, during AR and baseline after flight), and the “Grand Mean” of the set. Notice the similarity with the results from Koenig et al. (2002) and Bréchet et al. (2019)



mean template of these conditions (Grand Mean). Among these sets of templates, we noticed that topographies with similar labels resembled one another, regardless of the numbers of classes, and conditions and that these results have similarities with the literature. In Figure 5 we display the results related to six (6) classes, and templates corresponding to five (5) and four (4) classes are provided in the supplementary material (Figures S1 and S3). It is also noteworthy that the templates sustain a large correlation between themselves (Table S2).

Data-driven estimates indicated that the optimal number of clusters for the entire data (RSPre, Flight and RSpos) was four (4) classes. When only the Flight data was considered, the optimal number decreased to three (3) classes and it increased to five (5) when solely the baseline data (RSPre, RSpos) was accounted. A complete display of how the Global Explained Variance (GEV) and the Cross-validation criterion (CV) change with the number of clusters is attached in the supplementary material (Figure S6).

The hierarchical structure of our data hinders a proper display of microstate dynamic features (duration, occurrence, coverage and the transition matrix). Thus, for illustrative purposes, we simplified the features display by grouping each participant's datasets within similar conditions, and computed means and standard errors of the means as presented in Figure 6 and in the supplementary material (Figures S2 and S4). Nevertheless, we emphasize that for statistics, we used the linear mixed effects model, as described in Section 2.4.1.

For four classes, as presented in the Figure S2, our results suggested modulations of Classes 3 and 4 in flight in relation to rest:

All parameters (duration, occurrence and contribution) referring to Class 3 significantly decreased, while those of Class 4 increased. As for the five (Figure S4) and six classes (Figure 6), they both presented a significant decrease in all parameters (duration, occurrence and contribution) in similar topographies when we compared the data in flight with those obtained at rest (before and after flight). Interestingly, in our results, the topography associated with significant modulations on the dynamic features resembled the Microstate D of Seitzman et al. (2017) and the Microstate F of Custo et al. (2017) and Bréchet et al. (2019). However, the decrease on the dynamic features observed in our work for class F was opposed to the increase in class D reported by both Bréchet et al. (2019) and by Seitzman et al. (2017) in an attentional task performed in controlled environments.

Regarding the transition matrices, for four classes we noticed a distinct profile of transitions during flight in relation to data at rest: there was a greater likelihood that classes would transition to Microstate 4; and decreased likelihoods of Classes 1 and 2 transitioning to Class 3, and of Classes 3 and 4 to Class 1. However, for five and six microstate classes, we could not observe characteristic global patterns in the transition matrix.

### 3.3 | Source analysis

Finally, we performed a source reconstruction in Class F, that had significant modulations on the dynamic features. We display the



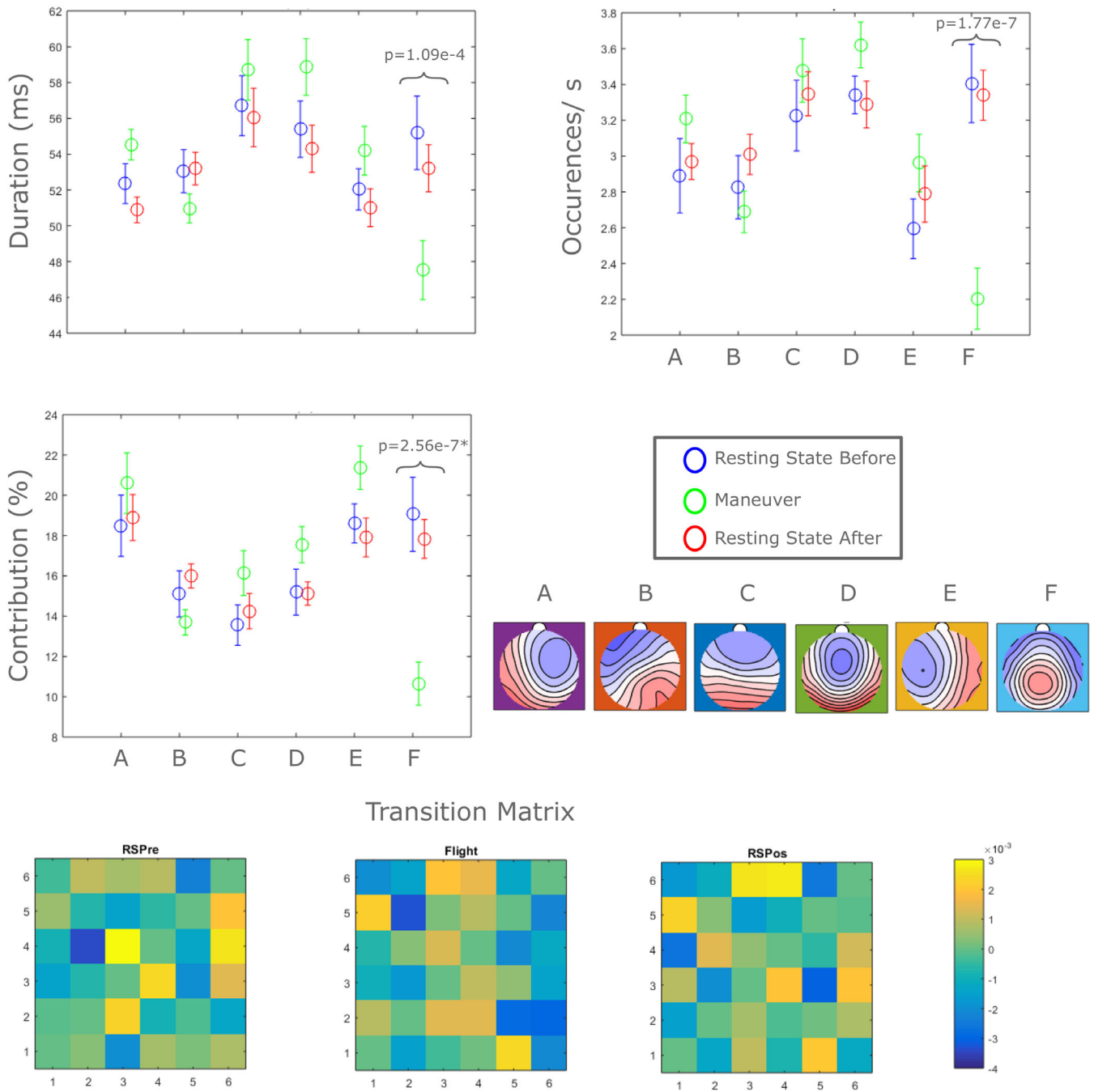


**FIGURE 6** Six classes microstate dynamics. Notice significant modulations in the parameters associated to the sixth class, with a topography resembling the Microstate D of Seitzman et al. (2017), and Microstate F of Custo, van der Ville, Wells, Tomescu, and Michel (2017) and Bréchet et al. (2019). The (\*) indicates that the residuals normality hypothesis was violated in the linear mixed effect model, and the statics was recalculated with the logarithmic operator in the dependent variable of Equation (1)

resultant of six classes, due to the resemblance of our templates with the ones from Bréchet et al. (2019). This work is particularly interesting not only due to the series of cognitive activities performed by the volunteers, but also due to their source reconstruction, that we used for comparison purposes. The Flight-RSPre contrast showed a cluster in the left prefrontal cortex ( $t(10) > 5.482, p < .05$ ) (Figure 7) after correction for multiple comparisons, encompassing Brodmann areas 11 and 47, with the peak (X, Y, Z) in the MNI coordinates corresponding to (-30, 30, -10).

#### 4 | DISCUSSION

The relevance of studies encompassing individuals in dynamic and complex environments is to further understand the relationship between decision-making and performance. In particular, we stress the importance of more accurately assessing the cognitive strategies at play during each moment, leading to a better understanding of how the SA is built and, mainly, how/if this information is useful for the design of safer and more reliable equipment and procedures

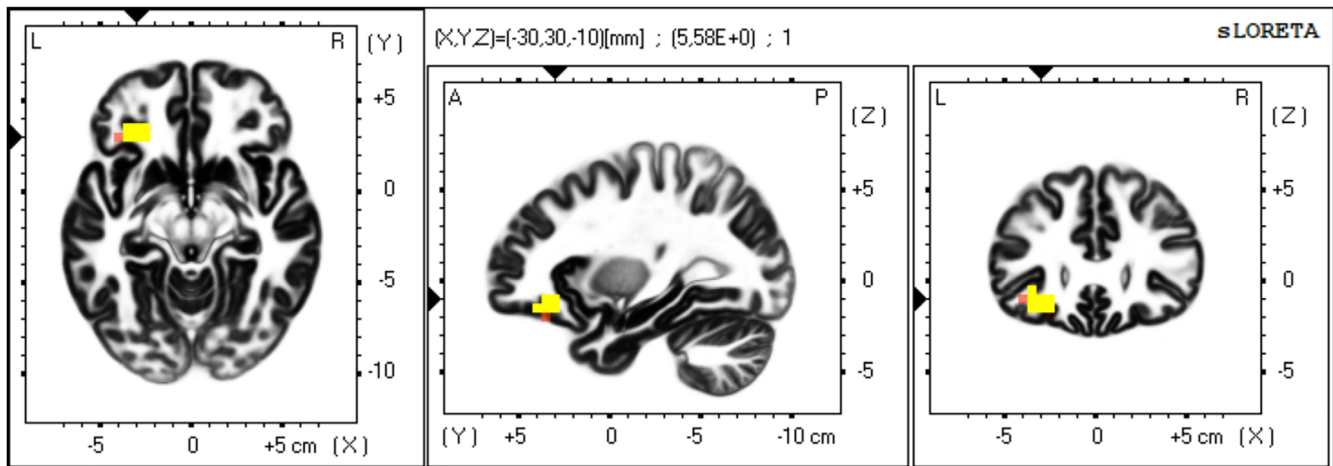


**FIGURE 7** Sources recovered through sLORETA for the Flight-RSPre contrast after the application of a paired  $t$  test ( $p < .05$ ), which pointed to a cluster in the left prefrontal cortex, in yellow, corresponding to greater activity in flight in relation to baseline

(Endsley, 2000). In this work, we explored the electrophysiology of decision making in an environment of this category. The results presented here are, to the best of our knowledge, unprecedented in the literature, since ecological studies with the EEG are scarce. Our results indicate that microstates are feasible neural correlates in an intrinsically noisy environment, strengthening and expanding the technique's horizon of application for studying cognition in more realistic conditions.

#### 4.1 | Microstates are feasible neural correlates even in extreme conditions

One of the major challenges of employing EEG data within a dynamic and complex environment comes from the high susceptibility of the signal to artifacts (Islam, Rastegarnia, & Yang, 2016). Nevertheless, there is evidence demonstrating that enhanced processing and filtering strategies produce a viable signal even in challenging environments, the main example being the simultaneous EEG and fMRI acquisitions (Ritter, Becker, Freyer, & Villringer, 2010). Our results add to this set of evidence by demonstrating the viability of EEG signals for microstate analyses in an ecological scenario.

However, we emphasize that not all data could be recovered: many epochs were contaminated by artifacts without a characteristic spectral signature, which made their removal unfeasible and, consequently, restricted our analyses to smaller windows. Movement artifacts were the most common due to the very nature of the piloting activity, which requires constant communication between the crew and the command tower. We chose the ICA as a strategy to handle artifacts due to its wide usability in signal preprocessing (Delorme & Makeig, 2004; Ritter et al., 2010; Soares et al., 2016), especially in microstate pipelines (Michel & Koenig, 2018), in addition to its effectiveness in indicating spurious sources (Hyvärinen & Oja, 2000), such as exemplified in Figure 4. Our environment was intrinsically noisy, forcing us to exclude a greater number of ICs (Refer to Table S1).

Nevertheless, removing an IC reduces the dimensionality of the data set likewise the removal of a channel, and the evidence indicating that the microstate model remains robust to a reduction in the number of EEG channels (Khanna, Pascual-Leone, & Farzan, 2014), led us to suppose that the pipeline would similarly accommodate a dimensionality reduction of the input signal.

Furthermore, the microstate analysis assumes that each topography is a correlate of the simultaneous activity of a set of networks in the brain, which functionally interact for a period of time, and that some characteristic topographies are recurrent over time (Koenig et al., 2002). This premise motivates the application of clustering algorithms for calculating topography templates, followed by the a posteriori classification of the data. Consequently, the attribution of each instant to one of the pre-defined classes disregards momentary variations, favoring a globally observable pattern. Thus, the microstate analysis embeds features that increase the robustness to external noise.

Our results support the effectiveness of the adopted artifact removal approach, since the template topographies recovered in flight are similar to those characterized for the same participants at rest in two distinct moments (Figure 5 and Figures S1 and S3). Moreover, they resemble other reports in the literature (Bréchet et al., 2019; Custo et al., 2017; Koenig et al., 2002; Pedroni et al., 2017; Seitzman et al., 2017). Nevertheless, we emphasize that although they largely correlate with each other (Table S2) there is a statistically significant difference from these topographies (even when solely resting state epochs are evaluated) when they are compared with the traditional topographic analysis of variance (TANOVA) (Koenig et al., 2011) (Figure S5).

In addition to that, there are other evidence pointing to the reliability of our data, such as the high internal consistency between two randomly defined subsets of all maneuvers, as detailed in the supplementary material (Table S3). It is also noteworthy that on a population level there was no difference on the microstates' modulations between the baseline recordings performed before and after the flight

(RSpre and RSpes) (as can be seen in Figure 6, Figures S2 and S4), which indicates that our recordings remained reliable after the flight. Although there was likely a difference on the pilots' mental activity on before and after the flight due to a multitude of factors that could impact brain dynamics, such as arousal, stress, nervousness, tiredness among others, they did not influence microstates' dynamic parameters.

In short, our results suggest that microstates are promising neural correlates in realistic situations, since they could be successfully recovered during an overly complex task in a hostile environment.

Finally, we emphasize that there are many approaches for artifact handling and validating this step is of extreme importance, especially under unusual experimental conditions, due to the particularities and nonlinearities of the EEG. We believe that, whenever possible, the usage of pre-established guidelines and pipelines for signal processing should be encouraged, as it allows the comparison with previous works.

## 4.2 | Microstate modulation in an ecological experiment: A comparison with controlled conditions

In this work, we explored the synergy between functional networks during a decision-making task, through the dynamic features of microstates. The usage of this type of analysis in cognitive tasks and establishing a relationship between these neural correlates with mental contents is still a recent field in the literature and our goal is to expand the horizons of applications to realistic scenarios.

The microstate dynamics is heavily dependent on the set of templates used for data backfitting. There is a compromise between maximizing the total variance that a set of topographies explains (specificity) and its generality at the group level (Michel & Koenig, 2018; Murray, Brunet, & Michel, 2008). Thus, templates at the individual level, that is, calculated exclusively from the participant data; at group level, considering all participants; and using a normative reference gradually increase generality and decrease specificity. As we aimed to characterize a peculiar population in an unusual condition, we opted for a balance between these options, computing templates at group level, employing data from our participants and using as few topographies as possible. This approach went against our initial expectation of recovering the four canonical topographies, for purposes of greater comparison with the literature, as can be seen in Figure S1. The dissimilarity from the canonical templates are likely due to the striking differences in the experimental conditions. The canonical microstates were usually computed with participants at rest and with their eyes closed. Nevertheless, our results were remarkably similar to the topographies of Pedroni et al. (2017) (Figure S1).

Pedroni et al. (2017) evaluated microstate dynamics during a gambling task, which enabled us to establish relations between risk taking in a controlled experiment versus a real scenario. The authors associated risk taking with the modulation of two microstates: the mean duration of Microstate 1 increased after the participant lost the bet and was associated with risk mitigation in the next trial. By contrast, the mean duration of Microstate 4 increased after successful bets,

being further related to greater risk acceptance. We also observed an antagonistic modulation of two microstates when we compared flight and baseline dynamics (Figure S1). However, these differences emerged between Classes 3 and 4. Therefore, our results corroborated with Pedroni et al., 2017 regarding the modulation of Microstate 4, reinforcing the association of this class with the preparation for a risky activity, in spite of the distinctive experimental conditions. We were not expecting a modulation in Microstate 1, likewise the reported by the authors given that, for our participants, risk aversion was not an option. However, the modulation in Microstate 3 was unexpected.

Given the lack of consensus in the total number of microstate classes, especially due to ambiguities when labeling canonical microstates C and D (Michel & Koenig, 2018), we further explored the variability of our results, using 5 and 6 classes. Increasing the number of classes led to templates resembling the normative reference of Koenig et al. (2002) and the work of Bréchet et al. (2019), as shown in Figure S3 and Figure 5, hence recovering the four canonical topographies (A–D), known in the literature. Our initial hypothesis was that decision making during the execution of the AR maneuver was mediated by attention and cognitive control networks, since pilots report a perceived workload increase during maneuver execution. Thus, we expected a significant modulation of parameters associated with the Microstate D, which was not observed in our work.

In our experiment, when contrasting flight with rest modulations for four (Figure S2), five (Figure S4) and six classes (Figure 6), we noticed a decrease in all dynamic parameters for the topography resembling the Microstate F of Custo et al. (2017) and of Bréchet et al. (2019). Furthermore, the topography is also similar to the microstate in which Seitzman et al. (2017) reported modulations during a mental subtraction task (in this article, classified as Microstate D). However, the authors reported an increase in class D parameters and a decrease in class C, while our results point to a decrease solely in Microstate F. Despite the differences in topography templates, the results of Bréchet et al. (2019) support Seitzman et al. (2017) regarding modulations in Classes C and D for the same mental subtraction task. Bréchet et al. (2019) further contrasted microstate modulations during mental computation not only with a baseline, but also with a memory recall task and matched EEG source reconstruction locations with high resolution fMRI records. However, it is noteworthy that in none of the three experimental conditions the authors reported modulation associated with topography F, as verified in our result.

The results of Custo et al. (2017) indicated that microstate classes have sources in common, and that if the number of classes is reduced there is a tendency for additional topographies to merge. From their data, 7 classes were computed, labeled from A to G, and the authors explored how grouping them into 4 classes justify some topography distortions in the canonical templates. According to them, there are also nuances regarding microstate labeling when more classes are considered: They reported that canonical class C (i.e., when only 4 classes are considered) is a combination of Classes C and F and that, in the literature, topographies classified as C may resemble either their topographies labeled as C or as F. Thus, their results suggest that, in

general, two topographies (C and F) are considered as representations of the same state and network when the number of classes decreases. Seitzman et al. (2017) reported a decrease in dynamic parameters associated with class C and argued that unlike the proposal of Britz et al. (2010), which associated this topography with the salience network, it should instead be related with the Default Mode Network (DMN) since this is the only task-negative network reported in the fMRI literature. In addition to that, Seitzman et al. (2017) also associated Microstate D with the dorsolateral attention network, which would corroborate with the increase they observed in dynamic parameters, since this network is task-positive. The findings of Bréchet et al. (2019) reinforce a functional association of class C with DMN and class D with networks in the prefrontal cortex.

The F topography of Custo et al. (2017) was associated to the anterior dorsal cortex (anterior cingulate cortex and the Broadman area 32), to bilateral areas in the frontal gyrus and in the insula. These results were corroborated and extended by Bréchet et al. (2019), that associated this class with the medial prefrontal cortex (mPFC) (bilateral). Our results point to congruence with these works, since the source reconstruction indicated a cluster of greater activity in the left prefrontal cortex during flight (Figure 7). The fact that our results are aligned with the literature becomes even more interesting when we consider the limitations of our setup: there is a significant decline in the source reconstruction quality when datasets have fewer electrodes (less than 32 channels) and that use a template for the head (Brodbeck et al., 2011). In addition, we had a relatively small number of participants.

Custo et al. (2017) stated that the mPFC is an area engaged in most classes of microstates and the authors interpret this region as a major hub in the integration of large-scale networks. In addition to that, the mPFC, and in particular its ventral part, is an important element in the emotional regulation circuit, in association with the amygdala (Buchanan et al., 2010; Etkin, Egner, & Kalisch, 2011; Marek, Strobel, Bredy, & Sah, 2013). Both regions have an influence on the hypothalamic-pituitary-adrenal axis, which, among other functions, are involved in stress reactions (Urry et al., 2006). The mPFC has a top-down modulation in the amygdala, that is, an increased activity in the mPFC leads to inhibitions in the amygdala activity and thus, it quickly attenuates the emotional response linked to negative events (Urry et al., 2006). This is in agreement with our results, that points to an increased activity in the mPFC during the maneuver (Figure 7) in comparison with the baseline. Nevertheless, notice that this microstate class has a significantly lower presence (duration, occurrence and contribution) in the decision-making epochs in relation to the baseline level. Therefore, our results indicate that when present, this microstate class has a higher activity on the mPFC, which modulates the limbic circuit. It is troublesome to make inferences about the overall effect on emotion-regulation circuits, but it may be indicative that decision making, in this case, is more associated with limbic responses, which might explain paralysis behaviors experienced by some pilots even after extensive training to refine their SA.

Nevertheless, given the exploratory nature of our study, we advise that such functional interpretations must be considered with caution. First, because we have not standardized pilot behavior immediately before/after maneuver execution, and, therefore, we lack in-flight baseline datasets that would allow us to characterize brain dynamics outside of the decision-making intervals. Thus, we are unable to guarantee that the modulation in Microstate F is due to the AR maneuver on itself and not a byproduct of other piloting activity. In addition to that, the microstate model considers cognition as a sequence of a finite number of brain states, and at any given moment only one of the networks is active. In practice, this is a simplification due to the overlap between some networks, and it is also worth mentioning that a portion of the signal variance is not covered by the model (Bréchet et al., 2019). Moreover, the microstate model has some open points that are relevant if one wants to employ this technique to further characterize SA, such as elucidating which systems are responsible for the dominance of a given class of microstate over the others and understanding the abrupt transition from one class to the next (Michel & Koenig, 2018). Finally, our results also reinforce that there may be more than four canonical microstates and corroborate reports that the cognitive manipulation of microstates is possible. Moreover, this work extends the horizon of experiments to more realistic and challenging conditions, since microstates seem to be robust neural correlates.

### 4.3 | Limitations and future work

Although the number of pilots in this work is significant compared to the number of experts at a global level (there is a small number of instructor training centers in the world [Wikipedia, 2019]), we still have few subjects to overcome the intrinsic variability of physiological measures. Therefore, we are still unable to establish direct and statistically representative relationships between microstate dynamics and each maneuver outcome or the participant expertise. Although in the aeronautical context the total number of maneuvers per participant is representative given the cost of a flight-test hour in a fully instrumented aircraft, this number of trials is still lower than what is usually performed in controlled physiology experiments. Balancing the constraints of these two distinct scenarios is one of the main challenges in processing data from realistic situations.

As new simulation and virtual reality technologies evolve, a new window of opportunity opens up for the study of SA, where some of the realism is compromised in favor of a cheaper study, which encompasses a larger number of participants and in a wider range of situations. For future studies, it would be interesting to evaluate pilots in flight simulators during different training stages—a longitudinal study.

Finally, we also emphasize the impact of noise. First, because the noise intrinsic to an experiment in these conditions is a risk, and the artifact-handling strategies may not result in viable EEG signals in all experimental contexts. Thus, it is important that every study in a new and challenging environment is preceded by feasibility analyses. In addition to that, noise characterization in unconstrained experimental

conditions is essential in order to allow the disentanglement of true neurophysiological effects from external contamination. In our experiment, had we previously recorded in-flight baselines, we would be able to further explore how residual noise influenced microstates' modulation. Therefore, we encourage that these epochs are included in other realistic experiments.

## ACKNOWLEDGMENTS

This project was supported by the Instituto de Pesquisas e Ensaio em Voos (IPEV), by the Coordenação de Aperfeiçoamento de Pessoal de Nível Superior (CAPES), Conselho Nacional de Desenvolvimento Científico e Tecnológico (CNPq), PROUNIEMP, and by IIEPAE.

## CONFLICT OF INTEREST

The authors declare no competing interest.

## AUTHOR CONTRIBUTIONS

Camila S. Deolindo performed physiological data recording, data analysis, and wrote the article; Mauricio W. Ribeiro and Maria A. A. de Aratanha performed physiological data recording and assisted data analysis; José R. S. Scarpari coordinated the flight campaign and analyzed aircraft mechanical data; Carlos H. Q. Forster analyzed aircraft mechanical data; Roberto G. A. da Silva supervised the aircraft data analysis; Birajara S. Machado, Edson Amaro Junior, and Elisa H. Kozasa supervised the physiological data analysis; Thomas König provided crucial insights into data analysis. All authors reviewed the article.

## DATA AVAILABILITY STATEMENT

Data to evaluate the results will be made available upon reasonable request to the corresponding author, through an agreement for data sharing.

## ORCID

Elisa H. Kozasa  <https://orcid.org/0000-0003-4723-6099>

## REFERENCES

- Bréchet, L., Brunet, D., Birot, G., Gruetter, R., Michel, C. M., & Jorge, J. (2019). Capturing the spatiotemporal dynamics of self-generated, task-initiated thoughts with EEG and fMRI. *NeuroImage*, *194*, 82–92. <https://doi.org/10.1016/j.neuroimage.2019.03.029>
- Bréchet, L., Brunet, D., Perogamvros, L., Tononi, G., & Michel, C. M. (2020). EEG microstates of dreams. *Scientific Reports*, (in press), *10*, 1–9. <https://doi.org/10.1038/s41598-020-74075-z>
- Britz, J., Díaz Hernández, L., Ro, T., & Michel, C. M. (2014). EEG-microstate dependent emergence of perceptual awareness. *Frontiers in Behavioral Neuroscience*, *8*, 163. <https://doi.org/10.3389/fnbeh.2014.00163>
- Britz, J., & Michel, C. M. (2011). State-dependent visual processing. *Frontiers in Psychology*, *2*, 370. <https://doi.org/10.3389/fpsyg.2011.00370>
- Britz, J., Van De Ville, D., & Michel, C. M. (2010). BOLD correlates of EEG topography reveal rapid resting-state network dynamics. *NeuroImage*, *52*, 1162–1170. <https://doi.org/10.1016/j.neuroimage.2010.02.052>
- Brodbeck, V., Spinelli, L., Lascano, A. M., Wissmeier, M., Vargas, M. I., Vulliemoz, S., ... Seeck, M. (2011). Electroencephalographic source imaging: A prospective study of 152 operated epileptic patients. *Brain*, *134*(10), 2887–2897. <https://doi.org/10.1093/brain/awr243>
- Buchanan, T. W., Driscoll, D., Mowrer, S. M., Sollers, J. J., Thayer, J. F., Kirschbaum, C., & Tranel, D. (2010). Medial prefrontal cortex damage affects physiological and psychological stress responses differently in men and women. *Psychoneuroendocrinology*, *35*(1), 56–66. <https://doi.org/10.1016/j.psyneuen.2009.09.006>
- Charles, R. L., & Nixon, J. (2019). Measuring mental workload using physiological measures: A systematic review. *Applied Ergonomics*, *74*, 221–232. <https://doi.org/10.1016/j.apergo.2018.08.028>
- Custo, A., van der Ville, D., Wells, W. M., Tomescu, I. M., & Michel, C. (2017). EEG resting-state networks: Microstates' source localization. *Brain Connectivity*, *7*(10), brain.2016.0476. <https://doi.org/10.1089/brain.2016.0476>
- da Cruz, J. R., Favrod, O., Roinishvili, M., Chkonia, E., Brand, A., Mohr, C., ... Herzog, M. H. (2020). EEG microstates are a candidate endophenotype for schizophrenia. *Nature Communications*, *11*(1), 1–11. <https://doi.org/10.1038/s41467-020-16914-1>
- Delorme, A., & Makeig, S. (2004). EEGLAB: An open source toolbox for analysis of single-trial EEG dynamics including independent component analysis. *Journal of Neuroscience Methods*, *134*(1), 9–21. <https://doi.org/10.1016/j.jneumeth.2003.10.009>
- Dierks, T., Jelic, V., Julin, P., Maurer, K., Wahlund, L. O., Almkvist, O., ... Winblad, B. (1997). EEG-microstates in mild memory impairment and Alzheimer's disease: Possible association with disturbed information processing. *Journal of Neural Transmission*, *104*(4–5), 483–495. <https://doi.org/10.1007/BF01277666>
- Endsley, M. R. (1995). Toward a theory of situation awareness in dynamic systems. *Human Factors: The Journal of the Human Factors and Ergonomics Society*, *37*(1), 32–64. <https://doi.org/10.1518/001872095779049543>
- Endsley, M. R. (2000). Theoretical underpinnings of situational awareness: A critical review. *Situation Awareness Analysis and Measurement*, *1*, 24. <https://doi.org/10.1177/1555343415572631>
- Endsley, M. R., & Garland, D. J. (2000). *Situation awareness analysis and measurement*. Boca Raton, FL: CRC Press.
- Etkin, A., Egner, T., & Kalisch, R. (2011). Emotional processing in anterior cingulate and medial prefrontal cortex. *Trends in Cognitive Sciences*, *15*(2), 85–93. <https://doi.org/10.1016/j.tics.2010.11.004>
- Federal Aviation Administration, U. (2016). *Helicopter flying handbook* (tech. rep.). Retrieved from [https://www.faa.gov/regulations\\_policies/handbooks\\_manuals/aviation/helicopter\\_flying\\_handbook/](https://www.faa.gov/regulations_policies/handbooks_manuals/aviation/helicopter_flying_handbook/).
- Hyvärinen, A., & Oja, E. (2000). Independent component analysis: Algorithms and applications. *Neural Networks*, *13*, 411–430. [https://doi.org/10.1016/S0893-6080\(00\)00026-5](https://doi.org/10.1016/S0893-6080(00)00026-5)
- Islam, M. K., Rastegarnia, A., & Yang, Z. (2016). Methods for artifact detection and removal from scalp EEG: A review. *Neurophysiologie Clinique/Clinical Neurophysiology*, *46*(4–5), 287–305. <https://doi.org/10.1016/j.neucli.2016.07.002>
- Jingze, Q. (2011). From autorotation to safe landing. *Procedia Engineering*, *17*, 46–51. <https://doi.org/10.1016/j.proeng.2011.10.006>
- Johnson, W. (2012). *Helicopter theory*. New York, NY: Courier Corporation.
- Katayama, H., Gianotti, L. R. R., Isotani, T., Faber, P. L., Sasada, K., Kinoshita, T., & Lehmann, D. (2007). Classes of multichannel EEG microstates in light and deep hypnotic conditions. *Brain Topography*, *20*(1), 7–14. <https://doi.org/10.1007/s10548-007-0024-3>
- Khanna, A., Pascual-Leone, A., & Farzan, F. (2014). Reliability of resting-state microstate features in electroencephalography. *PLoS One*, *9*(12), 1–21. <https://doi.org/10.1371/journal.pone.0114163>
- Khanna, A., Pascual-Leone, A., Michel, C. M., & Farzan, F. (2015). Microstates in resting-state EEG: Current status and future directions. *Neuroscience and Biobehavioral Reviews*, *49*, 105–113. <https://doi.org/10.1016/j.neubiorev.2014.12.010>
- Kinoshita, T., Strik, W. K., Michel, C. M., Yagyu, T., Saito, M., & Lehmann, D. (1995). Microstate segmentation of spontaneous multichannel EEG map series under diazepam and sulpiride. *Pharmacopsychiatry*, *28*(2), 51–55. <https://doi.org/10.1055/s-2007-979588>

- Koenig, T., Kottlow, M., Stein, M., & Melie-García, L. (2011). Ragú: A free tool for the analysis of EEG and MEG event-related scalp field data using global randomization statistics. *Computational Intelligence and Neuroscience*, 2011, 1–14. <https://doi.org/10.1155/2011/938925>
- Koenig, T., Lehmann, D., Merlo, M. C. G., Kochi, K., Hell, D., & Koukkou, M. (1999). A deviant EEG brain microstate in acute, neuroleptic-naive schizophrenics at rest. *Journal of Neural Transmission*, 249(4), 205–211.
- Koenig, T., Prichep, L., Lehmann, D., Sosa, P. V., Braeker, E., Kleinlogel, H., ... John, E. R. (2002). Millisecond by millisecond, year by year: Normative EEG microstates and developmental stages. *NeuroImage*, 16(1), 41–48. <https://doi.org/10.1006/nimg.2002.1070>
- Lancaster, J. L., Woldorff, M. G., Parsons, L. M., Liotti, M., Freitas, C. S., Rainey, L., ... Fox, P. T. (2000). Automated Talairach Atlas labels for functional brain mapping. *Human Brain Mapping*, 10(3), 120–131. [https://doi.org/10.1002/1097-0193\(200007\)10:3<120::AID-HBM30>3.0.CO;2-8](https://doi.org/10.1002/1097-0193(200007)10:3<120::AID-HBM30>3.0.CO;2-8)
- Lehmann, D., Ozaki, H., & Pal, I. (1987). EEG alpha map series: Brain microstates by space-oriented adaptive segmentation. *Electroencephalography and Clinical Neurophysiology*, 67(3), 271–288. <http://www.ncbi.nlm.nih.gov/pubmed/2441961>
- Marek, R., Strobel, C., Bredy, T. W., & Sah, P. (2013). The amygdala and medial prefrontal cortex: Partners in the fear circuit. *Journal of Physiology*, 591(10), 2381–2391. <https://doi.org/10.1113/jphysiol.2012.248575>
- Mazziotta, J., Toga, A., Evans, A., Fox, P., Lancaster, J., Zilles, K., ... Mazoyer, B. (2001). A probabilistic atlas and reference system for the human brain: International Consortium for Brain Mapping (ICBM). *Philosophical Transactions of the Royal Society B: Biological Sciences*, 356(1412), 1293–1322. <https://doi.org/10.1098/rstb.2001.0915>
- Michel, C. M., & Koenig, T. (2018). EEG microstates as a tool for studying the temporal dynamics of whole-brain neuronal networks: A review. *NeuroImage*, 180, 577–593. <https://doi.org/10.1016/j.neuroimage.2017.11.062>
- Milz, P., Faber, P. L., Lehmann, D., Koenig, T., Kochi, K., & Pascual-Marqui, R. D. (2016). The functional significance of EEG microstates-associations with modalities of thinking. *NeuroImage*, 125, 643–656. <https://doi.org/10.1016/j.neuroimage.2015.08.023>
- Müller, T. J., Koenig, T., Wackermann, J., Kalus, P., Fallgatter, A., Strik, W., & Lehmann, D. (2005). Subsecond changes of global brain state in illusory multistable motion perception. *Journal of Neural Transmission*, 112(4), 565–576. <https://doi.org/10.1007/s00702-004-0194-z>
- Murray, M. M., Brunet, D., & Michel, C. M. (2008). Topographic ERP analyses: A step-by-step tutorial review. *Brain Topography*, 20(4), 249–264. <https://doi.org/10.1007/s10548-008-0054-5>
- Nichols, T. E., & Holmes, A. P. (2002). Nonparametric permutation tests for functional neuroimaging: A primer with examples. *Human Brain Mapping*, 15(1), 1–25. <https://doi.org/10.1002/hbm.1058>
- Panda, R., Bharath, R. D., Upadhyay, N., Mangalore, S., Chennu, S., & Rao, S. L. (2016). Temporal dynamics of the default mode network characterize meditation-induced alterations in consciousness. *Frontiers in Human Neuroscience*, 10, 1–12. <https://doi.org/10.3389/fnhum.2016.00372>
- Pascual-Marqui, R. D., Michel, C. M., & Lehmann, D. (1995). Segmentation of brain electrical activity into microstates; model estimation and validation. *IEEE Transactions on Biomedical Engineering*, 42(7), 658–665. <https://doi.org/10.1109/10.391164>
- Pedroni, A., Gianotti, L. R., Koenig, T., Lehmann, D., Faber, P., & Knoch, D. (2017). Temporal characteristics of EEG microstates mediate trial-by-trial risk taking. *Brain Topography*, 30(1), 149–159. <https://doi.org/10.1007/s10548-016-0539-6>
- Poulsen, A. T., Pedroni, A., Langer, N., & Hansen, L. K. (2018). Microstate EEGlab toolbox: An introductory guide. *bioRxiv*, 1–30. <https://doi.org/10.1101/289850>
- Rieger, K., Hernandez, L. D., Baenninger, A., & Koenig, T. (2016). 15 years of microstate research in schizophrenia – Where are we? A meta-analysis. *Frontiers in Psychiatry*, 7, 1–7. <https://doi.org/10.3389/fpsy.2016.00022>
- Ritter, P., Becker, R., Freyer, F., & Villringer, A. (2010). In C. Mulert & L. Lemieux (Eds.), *EEG – fMRI: Physiological basis, technique, and applications*. Berlin Heidelberg: Springer. <https://doi.org/10.1007/978-3-540-87919-0>
- Seitzman, B. A., Abell, M., Bartley, S. C., Erickson, M. A., Bolbecker, A. R., & Hetrick, W. P. (2017). Cognitive manipulation of brain electric microstates. *NeuroImage*, 146, 533–543. <https://doi.org/10.1016/j.neuroimage.2016.10.002>
- Soares, J. M., Magalhães, R., Moreira, P. S., Sousa, A., Ganz, E., Sampaio, A., ... Sousa, N. (2016). A Hitchhiker's guide to functional magnetic resonance imaging. *Frontiers in Neuroscience*, 10, 515. <https://doi.org/10.3389/fnins.2016.00515>
- Strik, W. K., Chiaramonti, R., Muscas, G. C., Paganini, M., Mueller, T. J., Fallgatter, A. J., ... Zappoli, R. (1997). Decreased EEG microstate duration and anteriorisation of the brain electrical fields in mild and moderate dementia of the Alzheimer type. *Psychiatry Research – Neuroimaging*, 75(3), 183–191. [https://doi.org/10.1016/S0925-4927\(97\)00054-1](https://doi.org/10.1016/S0925-4927(97)00054-1)
- The United States Joint Helicopter Safety Analysis Team. (2011). *The Compendium report: The U.S. JHSAT baseline of helicopter accident analysis*. Retrieved from [https://jayc3.sg-host.com/Reports/US\\_JSHAT\\_Compendium\\_Report1.pdf](https://jayc3.sg-host.com/Reports/US_JSHAT_Compendium_Report1.pdf).
- The United States Joint Helicopter Safety Analysis Team. (2014a). *Comparative report*, Volume 2. Retrieved from <https://jayc3.sghost.com/Reports/Comparative%20Accident%20Report%20Vol%202.pdf>.
- The United States Joint Helicopter Safety Analysis Team. (2014b). *Comparative report: U.S. JHMDAT data to U.S. JHSAT data*. Retrieved from [https://jayc3.sg-host.com/Reports/US\\_JSHAT\\_Compendium\\_Report1.pdf](https://jayc3.sg-host.com/Reports/US_JSHAT_Compendium_Report1.pdf).
- Urry, H. L., Van Reekum, C. M., Johnstone, T., Kalin, N. H., Thuro, M. E., Schaefer, H. S., ... Davidson, R. J. (2006). Amygdala and ventromedial prefrontal cortex are inversely coupled during regulation of negative affect and predict the diurnal pattern of cortisol secretion among older adults. *Journal of Neuroscience*, 26(16), 4415–4425. <https://doi.org/10.1523/JNEUROSCI.3215-05.2006>
- Van De Ville, D., Britz, J., & Michel, C. M. (2010). EEG microstate sequences in healthy humans at rest reveal scale-free dynamics. *Proceedings of the National Academy of Sciences*, 107(42), 18179–18184. <https://doi.org/10.1073/pnas.1007841107>
- Wikipedia. (2019). *List of test pilot schools*. Retrieved from [https://en.wikipedia.org/wiki/List\\_of\\_test\\_pilot\\_schools](https://en.wikipedia.org/wiki/List_of_test_pilot_schools).
- Wilkinson, G. N., & Rogers, C. E. (1973). Symbolic description of factorial models for analysis of variance. *Applied Statistics*, 22(3), 392. <https://doi.org/10.2307/2346786>

## SUPPORTING INFORMATION

Additional supporting information may be found online in the Supporting Information section at the end of this article.

**How to cite this article:** Deolindo CS, Ribeiro MW, de Aratana MAA, et al. Microstates in complex and dynamical environments: Unraveling situational awareness in critical helicopter landing maneuvers. *Hum Brain Mapp*. 2021;42: 3168–3181. <https://doi.org/10.1002/hbm.25426>